Effect of elastic anisotropy on contact stiffness in resonance ultrasound microscopy

Jiayong Tian[a)]
Graduate School of Engineering Science, Osaka University, Machikaneyama 1-3, Toyonaka, Osaka 560-8531, Japan and Institute of Crustal Dynamics, Chinese Earthquake Administration, Subbox 28, Beijing P.O. Box 2855, Beijing 100085, People's Republic of China

Hirotsugu Ogi and Masahiko Hirao
Graduate School of Engineering Science, Osaka University, Machikaneyama 1-3, Toyonaka, Osaka 560-8531, Japan

(Received 28 April 2005; accepted 20 September 2005; published online 9 November 2005)

The classical Hertzian-contact theory for an isotropic material has been adopted to simplify quantitative evaluation of local elastic modulus by resonance-ultrasound microscopy (RUM). However, the validity of this simplified model must be confirmed because most materials show elastic anisotropy in small regions. This study investigates the influence of the elastic anisotropy of the tip and the specimen on the determination of the local elastic modulus in RUM by introducing the Hertzian-contact stiffness for orthorhombic materials. Numerical results reveal that specimen anisotropy significantly affects the contact stiffness and the quantitative evaluation of local elastic modulus even for specimens with weak anisotropy when we consider the anisotropy of the oscillator tip in RUM. © *2005 American Institute of Physics*. [DOI: 10.1063/1.2131201]

Evaluation of elastic properties in a micro- and nanoscale region of materials is of great importance for optimization of applications including surface-wave acoustic devices and microelectromechanical systems, which can be achieved by using nanoidentation and atomic force acoustic microscopy (AFM). In nanoindentation, the depth and the loading during the unloading process of an indenter are recorded to determine the elastic modulus, which is modeled as a contact problem of a flat rigid punch on an elastic half space.[1] In AFM, resonance-frequency shift of a vibrating cantilever contacting materials through a small tip is used to determine the elastic modulus, however, the resonant frequency is highly affected by the ambiguous gripping condition of the cantilever, quantitative evaluation of a material's elasticity has not been straightforward.[2,3] Recently, resonance-ultrasound microscopy (RUM) was developed as an alternative method of AFM.[4,5] An isolated oscillator contacts the specimen surface through a spherical tip. The mechanical constraint causes a resonance-frequency shift of the oscillator only depending on contact stiffness at the tip-to-specimen interface, which in turn depends on the elastic constants of the specimen and the tip in the contacting area. To date, the tip-to-specimen contact in AFM and RUM is often modeled as a contact problem of a sphere on an elastically isotropic half space based on classical Hertzian-contact theory. However, the tip and the specimen usually exhibit elastic anisotropy in microscale and nanoscale regions. For example, a polycrystalline material with no texture macroscopically shows elastic isotropy, but it shows elastic anisotropy in a small-scale region because of different orientations of individual grains. In nanoindentation, AFM and RUM, the contact radius is usually much smaller than the grain size. In nanoindentation, Vlassak *et al.* have considered the influence of specimen anisotropy on the indentation modulus by modeling a contact problem of a flat rigid punch on an elastically anisotropic half space based on the assumption of the rigid indenter.[6,7] However, in AFM and RUM, we must consider the elastic anisotropy of the tip and the specimen in most cases. At present, the validity of Hertzian-contact model for isotropic materials used in RUM and AFM has not been confirmed in evaluating the elastic modulus quantitatively.

The objective of this letter is to evaluate the influence of the elastic anisotropy of the tip and the specimen on the determination of the elastic modulus in RUM/AFM by introducing Hertzian-contact stiffness for orthorhombic materials. Following Willis,[8] we derive the relationship between the normal force F_0 applied to the tip and the normal indentation δ_0 for the contact between the tip and specimen, both of which show orthorhombic symmetry, as show in the Appendix. The result is given by

$$\delta_0 = \frac{I_0}{8}\sqrt[3]{\frac{9F_0^2}{\pi^2 R I_1}}, \tag{1}$$

where R is the radius of the spherical tip. I_0 and I_1 are determined in terms of Green's functions given in the Appendix. The resonant vibration of the oscillator causes harmonic perturbations to the force and the indentation. We denote the time-dependent force and time-dependent indentation as F and δ, respectively, and determine the dynamic contact stiffness k_A by

$$k_A = \frac{F - F_0}{\delta - \delta_0}. \tag{2}$$

In the case that $F_0 \gg |F - F_0|$, substitution of Eq. (1) into Eq. (2) yields an expression for k_A,

$$k_A \approx 4\sqrt[3]{\frac{3F_0 R\pi^2 I_1}{I_0^3}}. \tag{3}$$

The anisotropic tip-to-specimen contact stiffness k_A is compared with the contact stiffness k_I derived from the Hertzian-contact theory for isotropic materials, which is conventionally used,[2–5] k_I is given by

a)Author to whom correspondence should be addressed; electronic mail: chenlitedtian@yahoo.com.cn

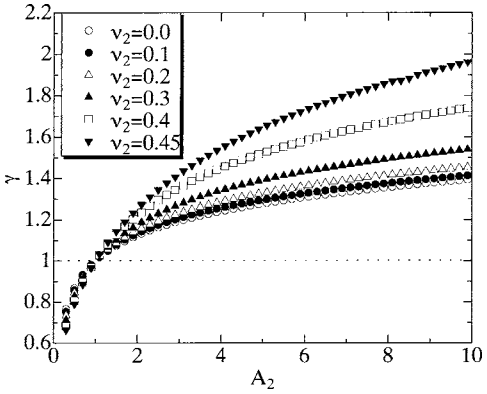

FIG. 1. The dependence of the contact-stiffness ratio γ on the anisotropy factor of the specimen A_2 when a spherical rigid tip touches (001) faces of cubic crystals with Poisson ratio ν_2.

$$k_I = \sqrt[3]{6E^{*2}RF_0}, \tag{4}$$

where $E^{*-1}=(1-\nu_1^2)E_1^{-1}+(1-\nu_2^2)E_2^{-1}$ is the effective Young's modulus. E_1, ν_1, E_2, and ν_2 represent Young's moduli and Poisson's ratios of the tip and the specimen along the normal direction to the contact surface, respectively.

Here, we consider that both the tip and specimen show cubic symmetry with three independent elastic constants. To represent the influence of the elastic anisotropy on the contact stiffness, we introduce the contact-stiffness ratio, $\gamma=k_A/k_I$. Thus, $\gamma=1$ verifies the isotropic Hertzian-contact approximation.

Figure 1 presents γ when a rigid tip contacts (001) faces of cubic crystals. γ is expressed as a function of the anisotropic factor $A_2[=2C_{44}/(C_{11}-C_{12})]$ and Poisson's ratio ν_2 of the cubic specimen. For all ν_2, $\gamma=1$ at $A_2=1$, indicating that the present anisotropic analysis contains the isotropic contact model [Eq. (4)]. We find that γ increases monotonically with the increase of A_2, which is the reverse of the results for the contact of a rigid punch on elastically anisotropic half space.[6] The dependence of γ on A_2 enhances as ν_2 increases. The isotropic contact stiffness differs from the anisotropic one by more than 20% for $A_2>2$ or $A_2<0.5$ when $\nu_2=0.4$; the isotropic contact-stiffness model is not valid for the evaluation of Young's modulus for (cubic) materials showing high elastic anisotropy.

We next investigate the influence of the tip's Young's modulus on the contact stiffness. We consider the case that (001) faces of the spherical cubic tip contacts the (001) face of the cubic specimen. We assume that $A_1=2$ and $\nu_1=\nu_2=0.3$. Figure 2 shows the dependence of γ on A_2 for three ratios of the normal Young's moduli of the tip and specimen.

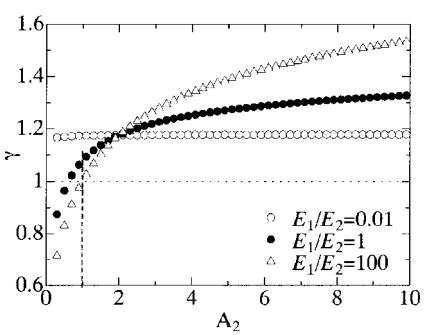

FIG. 2. The contact-stiffness ratio γ vs the anisotropy factor of the specimen A_2 when the (001) face of a spherical elastic tip contacts (001) faces of cubic crystals.

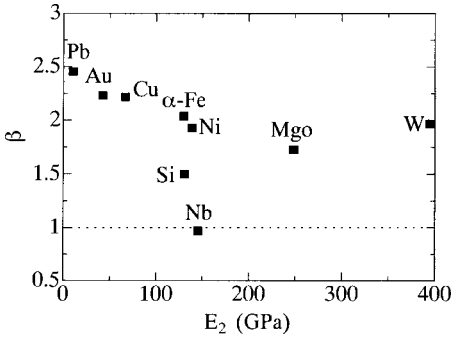

FIG. 3. The ratio β of the normal Young's moduli determined by the anisotropic and isotropic contact-stiffness models when the (001) face of a spherical silicon tip contacts the (001) faces of single cubic crystals.

(Normal Young's modulus means the Young's modulus along the ⟨001⟩ direction.) When the tip is much softer than the specimen, γ changes little with the specimen's anisotropy, A_2. When the tip is much stiffer than the specimen, γ naturally shows a similar behavior to the rigid-tip case (Fig. 1). Therefore, when the difference of Young's moduli of the tip and specimen is large, the contact stiffness k_A is principally governed by the elastic anisotropy of the material with the lower modulus.

Previous studies evaluated the local Young's modulus from the contact stiffness determined by the resonance-frequency shifts using the isotropic-contact-stiffness approximation.[2–5] This simple model, however, should involve the error caused by the elastic anisotropy. In order to estimate this error, we calculate the normal Young's modulus E_2' considering elastic anisotropy by replacing k_I in Eq. (4) with k_A in Eq. (3) and compare it with E_2, which is the normal Young's modulus along the ⟨100⟩ direction of the cubic specimen. Figure 3 presents $\beta=E_2'/E_2$ when the (001) face of a monocrystal silicon tip contacts (001) faces of the specimens. Here, we set $\nu_2=0.25$. For Pb, Au, Cu, α-Fe, and Ni,[9] which show high anisotropy ($A_2>2$), the estimated moduli are at least two times larger than the true moduli. Even for tungsten (W),[9] which shows $A_2\approx 1$, β nearly equals two because of the anisotropy of the silicon tip and the larger modulus of tungsten. Thus, we tend to overestimate the modulus of the specimen in RUM because of the elastic anisotropy of the tip and specimen.

We finally investigate the effect of the crystallographic orientation of the specimen on the contact stiffness. Figure 4 shows the ratios of the normal Young's moduli, the isotropic contact stiffnesses, and the anisotropic contact stiffnesses when a rigid tip contacts the (110) and (001) faces of cubic

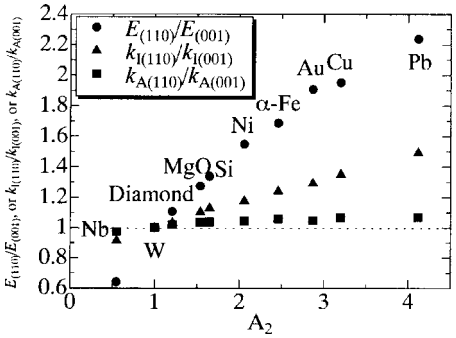

FIG. 4. Ratios of the normal Young's moduli, isotropic contact stiffnesses, and anisotropic contact stiffnesses for contacts with (110) and (100) faces of cubic crystals.

crystals. [Cubic crystals with (110) face exhibit orthorhombic symmetry.] The ratio of the normal Young's moduli $E_{(110)}/E_{(001)}$, along $\langle 110\rangle$ and $\langle 001\rangle$ directions increases from 0.64 (Nb) to 2.24 (Pb) as A_2 increases. The corresponding contact-stiffness ratio $k_{I(110)}/k_{I(001)}$ in the isotropic contact-stiffness model also increases from 0.91 (Nb) to 1.49 (Pb). However, the contact-stiffness ratio $k_{A(110)}/k_{A(001)}$ in the anisotropic contact-stiffness model varies only from 0.97 (Nb) to 1.067 (Pb). This means that the crystallographic orientation at the contacting surface has less influence on the contact stiffness: The resonant frequency of the oscillator is not very much affected by the grain orientation.

In summary, we considered the influence of the elastic anisotropy of the tip and the specimen on the determination of the local elastic modulus in RUM by introducing the Hertzian-contact stiffness for orthorhombic materials. The difference between the anisotropic and isotropic contact models is compared with various anisotropy factors and Poisson's ratios for both the tip and specimen. Numerical results strongly indicate that the elastic anisotropy of the tip and specimen must be considered for determining the local elastic modulus in RUM, even for materials with weak anisotropy. The elastic anisotropy tends to increase the contact stiffness and then the resonant frequency of the oscillator. However, the crystallographic orientation at the contact area has a relatively small influence on the contact stiffness and the resonant frequency compared with the elastic modulus, which induces smaller resonant-frequency shifts in the elastic-stiffness mapping on a polycrystalline material, even in the case where the normal Young's modulus strongly depends on the grain orientation. Therefore, if we evaluate the elastic modulus in different grain orientations, we need the accurate measurement of the resonant frequencies of the oscillator in RUM and then the accurate determination of contact stiffness from the measured resonant frequencies. This study also can be directly applied to the evaluation of elastic modulus in AFM and be helpful to nanoidentation measurements.

Willis[7] presented a general procedure to determine the contact radius and the indentation for orthorhombic materials, which is outlined in the following. Consider a biasing force F applied to a spherical tip with radius R to make it contact with a specimen surface. The specimen is a half space of a material having an orthorhombic elastic anisotropy. The tip is also assumed to be of an orthorhombic material with a principal axis normal to the specimen surface. Two Cartesian coordinates (x_1, y_1, z_1) and (x_1, y_1, z_2) relating with the tip and the specimen, respectively, have the origins at the center of the contacting area; the x_1-y_1 plane coincides with the tangential plane and the z_1 and z_2 axes are along the inward normal directions to the tip and the specimen at the contacting interface, respectively. Because of the orthorhombic anisotropy, the contact area has an elliptical shape with the semiaxes a_1 and a_2 in the x_1 and y_1 directions, respectively. The contact pressure distribution is expressed as

$$p(x_1,y_1) = p_0\left(1 - \frac{x_1^2}{a_1^2} - \frac{y_1^2}{a_2^2}\right)^{1/2}, \tag{5}$$

where p_0 is the maximum contact pressure at the center. p_0, a_1, and a_2 can be subsequently determined from the contact geometries.

The surface displacements for the tip and the specimen caused by the contact pressure are calculated from

$$w_\alpha(x_1,y_1) = \frac{3F}{16\pi a_1}\int_0^{2\pi} \hat{G}_\alpha(\varepsilon\eta_1,\eta_2)\left\{1 - \left(\frac{\eta_1 x_1}{a_1} + \frac{\eta_2 y_1}{a_2}\right)^2\right\} d\theta, \tag{6}$$

where $\alpha=1$ and 2 indicate the specimen and the tip, respectively. $\varepsilon = a_2/a_1$, $\eta_1 = \cos\theta$, $\eta_2 = \sin\theta$, and $F = 2p_0\pi a_1 a_2/3$. $\hat{G}_\alpha(x_1,y_1)$ denotes the Fourier transform of Green's function for surface displacements and involves the anisotropic elastic constants, which is expressed as[8]

$$G_\alpha(x_1,y_1) = \frac{1}{4\pi^2}\int\int \hat{G}_\alpha(\xi_1,\xi_2) e^{-i(\xi_1 x_1 + \xi_2 y_1)} d\xi_1 d\xi_2. \tag{7}$$

Considering the contact geometry condition for the tip-specimen within the contact area yields

$$\frac{I_2}{I_1} = \varepsilon^2, \tag{8a}$$

$$\delta = \frac{3FI_0}{16a_1\pi}, \tag{8b}$$

where ε is determined numerically by iterations[10]

$$I_0 = \sum_{\alpha=1}^{2}\int_0^{2\pi} \hat{G}_\alpha(\varepsilon\eta_1,\eta_2) d\theta,$$

$$I_1 = \sum_{\alpha=1}^{2}\int_0^{2\pi} \hat{G}_\alpha(\varepsilon\eta_1,\eta_2)\eta_1^2 d\theta,$$

$$I_2 = \sum_{\alpha=1}^{2}\int_0^{2\pi} \hat{G}_\alpha(\varepsilon\eta_1,\eta_2)\eta_2^2 d\theta.$$

After determining ε, the indentation δ is deduced as

$$\delta = \frac{I_0}{8}\sqrt[3]{\frac{9F^2}{\pi^2 R I_1}}. \tag{9}$$

The earlier equation shows that the indentation δ is proportional to $\sqrt[3]{F^2}$, which is the same as that in isotropic contact model.

This study was supported by Industrial Technology Research Grant Program in '04 from New Energy and Industrial Technology Development Organization (NEDO) of Japan.

[1] A. C. Fischer-Cripps, *Nanoindentation* (Springer, New York, 2002).
[2] K. Yamanaka and S. Nakano, Appl. Phys. A: Mater. Sci. Process. **66**, S313 (1998).
[3] U. Rabe, J. Turner, and W. Arnold, Appl. Phys. A: Mater. Sci. Process. **66**, S277 (1998).
[4] H. Ogi, J. Tian, T. Tada, and M. Hirao, Appl. Phys. Lett. **83**, 464 (2003).
[5] J. Tian, H. Ogi, T. Tada, and M. Hirao, J. Appl. Phys. **94**, 6472 (2003).
[6] J. J. Vlassak and W. D. Nix, Philos. Mag. A **67**, 1045 (1993).
[7] J. J. Vlassak, M. Ciavarella, J. R. Barber, and X. Wang, J. Mech. Phys. Solids **51**, 1701 (2003).
[8] J. R. Willis, J. Mech. Phys. Solids **14**, 163 (1966).
[9] G. Simmons and H. Wang, *Single Crystal Elastic Constants and Calculated Aggregate Properties: A Handbook*, 2nd ed. (MIT Press, Cambridge, MA, 1971).
[10] S. R. Swanson, Int. J. Solids Struct. **41**, 1945 (2004).